

Radical Anions of Oxidized vs. Reduced Oxytocin: Influence of Disulfide Bridges on CID and Vacuum UV Photo-Fragmentation

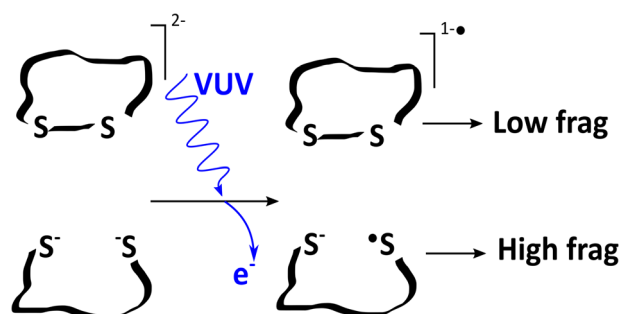
Luke MacAleese,¹ Marion Girod,² Laurent Nahon,³ Alexandre Giuliani,^{3,4}
Rodolphe Antoine,¹ Philippe Dugourd¹

¹Université de Lyon, CNRS, Université Claude Bernard Lyon 1, Institut Lumière Matière UMR 5306, 69622, Villeurbanne, France

²Université de Lyon, CNRS, Université Claude Bernard Lyon 1, ENS de Lyon, Institut des Sciences Analytiques UMR 5280, 69100, Villeurbanne, France

³Synchrotron SOLEIL, BP 48 St Aubin, 91192, Gif Sur Yvette, France

⁴UAR1008 CEPIA, INRA, BP 71627, 44316, Nantes, France



Abstract. The nonapeptide oxytocin (OT) is used as a model sulfur-containing peptide to study the damage induced by vacuum UV (VUV) radiations. In particular, the effect of the presence (or absence in reduced OT) of oxytocin's internal disulfide bridge is evaluated in terms of photo-fragmentation yield and nature of the photo-fragments. Intact, as well as reduced, OT is studied as dianions and radical anions. Radical anions are prepared and photo-fragmented in two-color

experiments (UV + VUV) in a linear ion trap. VUV photo-fragmentation patterns are analyzed and compared, and radical-induced mechanisms are proposed. The effect of VUV is principally to ionize but secondary fragmentation is also observed. This secondary fragmentation seems to be considerably enabled by the initial position of the radical on the molecule. In particular, the possibility to form a radical on free cysteines seems to increase the susceptibility to VUV fragmentation. Interestingly, disulfide bridges, which are fundamental for protein structure, could also be responsible for an increased resistance to ionizing radiations.

Keywords: Electron photo-detachment, Photo-fragmentation, Two-colors experiment, Disulfide bridge, Vacuum UV, Oxytocin, Radical peptide

Received: 7 March 2018/Revised: 27 April 2018/Accepted: 5 May 2018/Published Online: 12 June 2018

Introduction

The underlying processes in biomolecules activated by high-energy photons, in particular the vacuum UV/VUV radiation, are of tremendous importance in radiation science [1, 2]. Radical formation on biomolecules is often observed following high-energy photon irradiation, either due

to direct homolytic cleavage or to radical transfer involving solvent molecules [3]. Radical cations are important sources of damage to DNAs [4] and are major ingredients in photo-oxidation of proteins [5]. Phenoxy and indolyl radicals are ubiquitous in protein science: these radicals favor long-distance charge transport [6–9] and propagation of radical damage in proteins [10, 11]. For instance, tryptophan photolysis, through photoinduced electron transfer to nearby disulfide bridges, may induce disulfide reduction leading to a thiolate and a thiyl radical [12]. Thiyl radicals can also be produced via a direct light-induced homolysis of cystine disulfide bonds [13, 14]. Ultimately, thiyl radical-mediated damage to proteins may lead

Electronic supplementary material The online version of this article (<https://doi.org/10.1007/s13361-018-1989-8>) contains supplementary material, which is available to authorized users.

Correspondence to: Luke MacAleese; e-mail: luke.macaleese@univ-lyon1.fr

to protein aggregation and fragmentation, for example, in antibodies [15, 16]. Thus, probing photoprocesses in thiol radical-containing biomolecules activated by vacuum UV (VUV) radiation would help improving our knowledge in radiation damage science.

Electron capture or electron transfer approaches (ECD/ETD), applied to multiple protonated peptides, were widely reported to dissociate disulfide bridges into a thiol and a thiol radical [17]. Gas phase experiments using collision-induced dissociation coupled to ion trap mass spectrometry represent another useful approach to generate thiol radicals by dissociation of S-nitrosylated homocysteine compounds [18, 19]. Light can also be used to generate cysteine radicals from modified peptides in the gas phase [20]. A similar approach was used by Julian et al. with quinone-substituted cysteines, although, in this latter case, the photoinduced radical is located on cysteine C_β, and the sulfur is lost [21]. In a previous work, we reported vacuum UV spectroscopic investigations on phenoxy and indolyl radicals formed by direct irradiation of the non-modified peptide by UV laser pulses [22]. Neutral indolyl and phenoxy radicals were generated in the gas phase by using electron photo-detachment from WVVVV (and YVVVV) doubly deprotonated peptides, the C-terminal carboxyl group was a deprotonation site, and the second deprotonation occurred on the nitrogen of the indole (and the oxygen of tyrosine's phenol) ring. Electron detachment from this deprotonated ring led to the formation of an indolyl (and a phenoxy) radical, which were further irradiated by a VUV light using synchrotron radiation. Following the same two-colors experiment scheme, we aim at producing thiol radicals in a model sulfur-containing peptide anion and investigating their VUV-induced fragmentation.

In this study, we aimed at understanding the influence of disulfide bridges and their reduction on the stability of cysteine-containing peptides upon VUV irradiation. The formation of a radical by electron photo-detachment on a gas phase peptide results in specific fragmentation. But, while multiple mechanisms were proposed and tested in the case of radical cations, in particular the dissociation of disulfide bridges by ECD/ETD [17], much less is known from radical anions. The reason probably has to do with the higher instability of anions towards electron emission and spontaneous fragmentation brings some experimental complexity, while theoretical chemistry of negatively charged species is also very challenging, set aside the issue of radicals and unpaired electrons. In this study, we use oxytocin (OT) as a model sulfur-containing peptide. Oxytocin is a nonapeptide hormone with an internal disulfide bridge and amidated C-terminus, known to be active in various physiological processes and critical for cell-signaling mechanisms (Scheme 1) [23]. Photo-degradation in the UV range of oxytocin and the thermal stability of its

photoproducts have been studied by Mozziconacci and Schöneich in solution [24]. The formation, reactivity, and lifetime of disulfide radicals were also reported earlier in solution [25, 26]. In this study, we present results of VUV photofragmentation spectroscopy of radicals, generated from both oxidized and reduced forms of oxytocin isolated in the gas phase. Collision-induced dissociation (CID) and VUV patterns are compared in order to draw mechanistic conclusions. Several fragmentation schemes are proposed to explain the major features and differences between the VUV photo-dissociation spectra of reduced and non-reduced oxytocin. We discuss the initial position of the charge and the radical as a function of the presence of the disulfide bridge. We comment on the fragmentation patterns observed for oxytocin radical anions as a result of this initial radical position.

Experiments and Methods

Sample

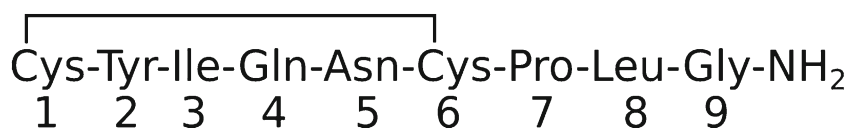
Oxytocin acetate salt hydrate (Sigma-Aldrich, St Quentin-Fallavier, France) was dissolved in water and diluted in acetonitrile (ACN), to reach a concentration of 30 μM in H₂O:ACN (1:1). OT is sold in its oxidized form (OTSS). In order to obtain the reduced form (OTSH), the reducing agent tris(2-carboxyethyl)phosphinehydrochloride (TCEP, Sigma-Aldrich) was added to the solution at a 10-fold excess with regard to oxytocin. The resulting OTSS/OTSH solutions were used as is in the ESI source of the mass spectrometers.

OT Singly Charged Anions: High-Resolution Mass Spectrometry

The CID spectra of singly charged anions ([OTSS]⁻ and [OTSH]⁻) were measured on a QExactive mass spectrometer (Thermo). The monoisotopic peaks at *m/z* 1005.429 and 1007.446 were selected with a window width of *m/z* 1 and activated in the HCD cell with collision energies (CE) ranging from 2 to 40 eV. The mass spectra presented below correspond to a CE of 40 eV. CID mass spectra were recorded on the mass range [75:1200] with a resolution of 140,000.

OT Dianions and Radicals: CID and VUV Photo-Dissociation

The CID spectra of oxytocin dianions (OTSS and OTSH) as well as their singly charged radical anion counterpart (OTSS and OTSH) were recorded in a LTQ XL linear ion trap mass spectrometer (Thermo). For CID, the dianions were mass selected (*m/z* 502 and 503 for OTSS and OTSH respectively) and activated with a “normalized collision energy” (NCE) of 15.



Scheme 1. Oxytocin sequence

The “Act Q” parameter was always kept at 0.25 (default) at all times. In order to generate radical anions, the mass-selected dianions were mass-isolated and subjected to 266-nm irradiation (4th harmonic of Nd:YAG, 6 mJ, 20 Hz, Brilliant A, Quantel). The dianions activation time was set to 600 ms, while keeping the NCE to 0. After irradiation at 266 nm, the radical anions formed by electron detachment are mass selected (window m/z 1) and activated with NCE ranging from 25 to 35.

Vacuum UV fragmentation of the dianions and radicals was recorded on the same instrument (LTQ XL) that is coupled [27] to the DESIRS beamline [28] at the SOLEIL synchrotron radiation facility (France). For the VUV photo-dissociation experiments for dianions and radicals, instead of applying collisional activation, NCE was set to 0 and the activation time was set to 600 ms during which the vacuum UV beam of the synchrotron was injected on axis in the LTQ ion trap on the selected ions (Scheme 2). Practical details of the UV and VUV combination (via a mirror with a central hole) and coupling to the mass spectrometer can be found in prior publications [29, 30]. The synchrotron beam, passing through a 500 μm monochromator slit, was filtered by an MgF2 window (below 9 eV) and an Ar-filled gas filter (8–16 eV) in order to suppress the high harmonics of the undulator. Thus, harmonic-free monochromatized VUV radiation was used to irradiate ions with a 12 meV bandwidth. The fragmentation ratios presented as inset in Figures 1, 2, 3, and 4 are defined as “ $1 - I_{\text{parent}}/\text{TIC}$ ”, with I_{parent} the intensity of the parent ion and TIC the total ion current. They are not corrected for the VUV photon flux (Figure S5).

Results

The VUV photo-dissociation spectra of oxidized and reduced OT dianions, as well as of their associated singly charged radical created by electron photo-detachment, were recorded over the 4.5 to 16 eV range.

Figures 1 and 2 present the VUV photo-dissociation mass spectra of respectively OTSS and OTSH dianions averaged over the whole VUV range. One major feature in both cases is electron detachment, yielding the radical anions [OTSS] $^{\cdot-}$ (m/z 1004) and [OTSH] $^{\cdot-}$ (m/z 1006). This initial electron detachment is followed by radical-induced fragmentation of the resulting radical anions, as described below.

In OTSS, the fragment ions observed at m/z 971.2 and m/z 939.3 could result from neutral losses of 33 and 65 Da corresponding to SH $^{\cdot}$ (Scheme S1) and S₂H $^{\cdot}$ (Scheme 3) from the radical precursor. These mechanisms require first the H abstraction from either Cys C $_{\alpha}$ or C $_{\beta}$ by the tyroxy radical, as previously reported by Beauchamp and coworkers [31], which is associated with the transfer of the radical on cysteine C $_{\alpha}$ or

C $_{\beta}$. This allows the radical-induced cleavage of the disulfide bridge and the radical elimination of SH $^{\cdot}$ and S₂H $^{\cdot}$. This latter loss suggests that in the OTSS radical, the disulfide bridge is conserved. Four other intense C-term fragments are observed at m/z 898.2, m/z 886.2, m/z 853.3, and m/z 369.1. These ions are observed in the CID spectrum of the radical anion (Figure S3), but not of the non-radical species (Figure S1). They are thus produced by radical-induced fragmentation. The m/z 898.2 ion could arise from the radical-induced elimination of the tyrosine sidechain (Scheme S2). This supports the hypothesis that the radical is initially formed on tyrosine. The ion detected at m/z 369.1 corresponds to fragment z₄ and could be produced, after H abstraction from Cys6 C $_{\beta}$, by the radical-induced cleavage of the N–C bond between Asn5 and Cys6, together with the 1,3 H transfer from the Cys1 C $_{\beta}$ to Cys6 sulfur (Scheme S3). When considering the H abstraction from Cys1 C $_{\beta}$, the radical-induced cleavage of the N–C bond of Tyr2 associated with the 1,3 H transfer from the Cys6 C $_{\beta}$ to Cys1 sulfur (Scheme 4) could yield the radical ion detected at m/z 886.2. Eventually, following H abstraction by the tyroxy radical from Cys6 C $_{\alpha}$, the ion at m/z 853.3 may arise from the radical-induced cleavage of Cys6 C $_{\beta}$ –S bond, concerted with the 1,3 H transfer from Tyr2 C $_{\beta}$ to Tyr2 backbone nitrogen (Scheme 5).

Remarkably, the relative intensity of the tyrosine sidechain loss is high in the VUV photo-dissociation (VUVPD) mass spectrum of the dianions while it is comparably lower in the CID spectrum of the OTSS radical in Figure S3. This supports the hypothesis that the radical created on the tyrosine is moving over the backbone: in the VUVPD of the OTSS dianion, fragmentation may occur immediately after the electron detachment, without radical scrambling due to collisional activation. Thus, the radical may remain localized longer on tyrosine, hence the favored local radical fragmentation pathway.

For the OTSH dianion (Figure 2), the loss of NH₃ and SH $^{\cdot}$ is predominant in the VUV photo-dissociation spectrum. Although NH₃ loss can also be reported in non-radical species, the intensity of those particular fragments is significantly enhanced in the CID spectrum of the radical species. Thus, it is hypothesized that they are both generated via radical-induced mechanisms (Scheme S4 and Scheme 6), in particular the loss of NH₃ which is specifically observed in the CID spectrum of the OTSH radical (Figure S4) but not of the non-radical anion (Figure S2). Two intense fragments are also observed on the VUVPD mass spectrum: b₅ and c₅. Fragment b₅ could originate from the radical-induced cleavage of the amide bond between Asn5 and Cys6 following the H abstraction on Asn5 C $_{\alpha}$ by radical sulfur on Cys6 (Scheme 7). Fragment c₅ could originate from the Cys6 N–C bond cleavage concerted with the S–O bond formation between Cys6 radical sulfur and carbonyl, and the 1,5 H transfer from Cys6 C $_{\beta}$ to Asn5 carbonyl (Scheme S5), similar to the mechanism reported for electron



Scheme 2. Two-colors (UV + VUV) sequence

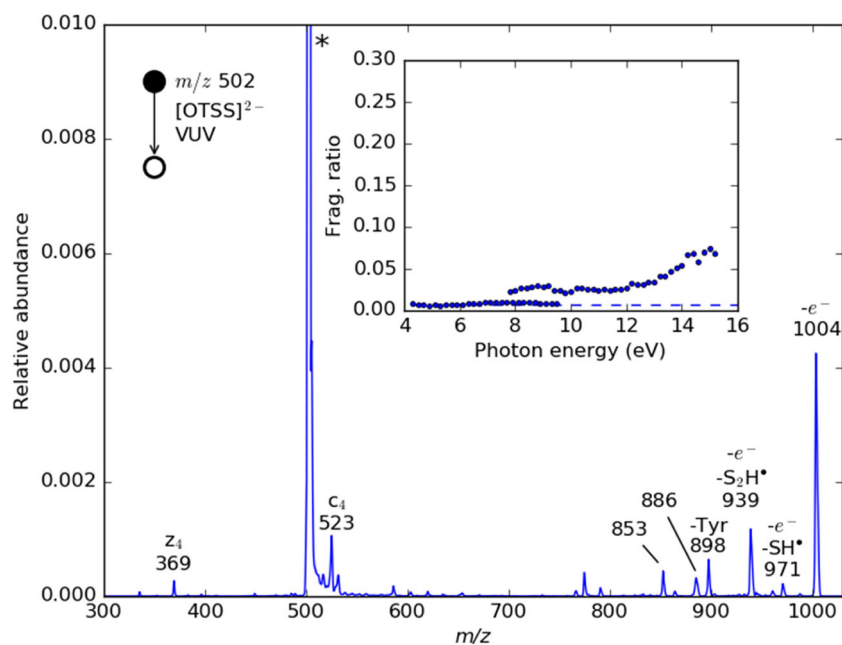


Figure 1. $[\text{OTSS}]^{2-}$ VUVPD mass spectrum averaged over the full 4.5 to 16 eV range. In inset, the evolution of the fragmentation ratio with the VUV photon energy (bullets), compared to the spontaneous fragmentation ratio (dashed line)

detachment dissociation on cysteine-containing peptides [32]. Interestingly, the NH_3 loss involves a radical on Cys1 whereas the b_5 and c_5 fragments involve a radical on Cys6. This suggests that the radical can be equally formed on both cysteines from OTSH dianion. In any case, this provides evidence for the formation of a thiyl radical upon VUV irradiation (and thus for the position of the charges on the free cysteines in the dianions). The fragmentation ratios of the dianions are similar:

weak, but increasing with the photon energy (see insets in Figures 1 and 2).

Figures 3 and 4 present the VUV photo-dissociation mass spectra of the radical anions formed by electron detachment from OT dianions: respectively $[\text{OTSS}]^{\cdot-}$ and $[\text{OTSH}]^{\cdot-}$. In contrast to dianions, electron photo-detachment leads to neutral species, which cannot be observed. Thus, the observed charged fragments result from a competition between fragmentation

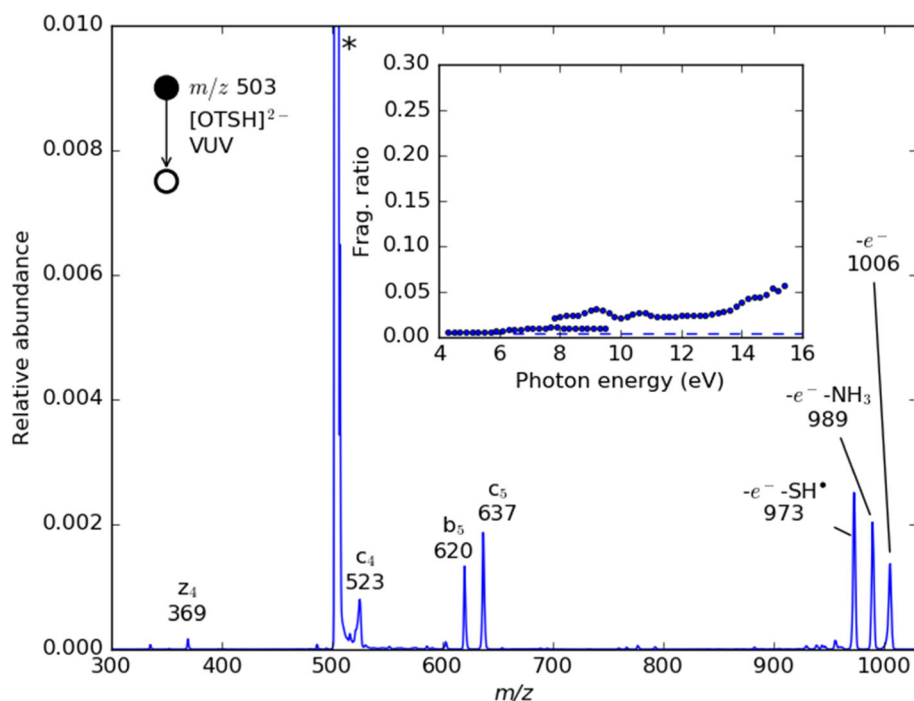


Figure 2. $[\text{OTSH}]^{2-}$ VUVPD mass spectrum averaged over the full 4.5 to 16 eV range. In inset, the evolution of the fragmentation ratio with the VUV photon energy (bullets), compared to the spontaneous fragmentation ratio (dashed line)

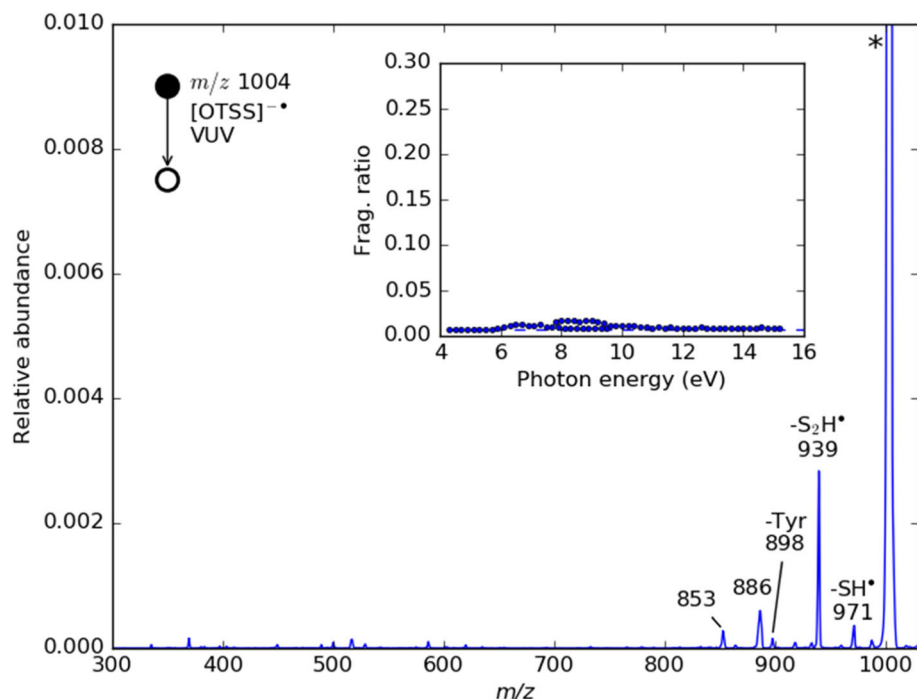


Figure 3. [OTSS]⁻ VUVPD mass spectrum averaged over the full 4.5 to 16 eV range. In inset, the evolution of the fragmentation ratio with the VUV photon energy (bullets), compared to the spontaneous fragmentation ratio (dashed line)

and photo-detachment. Nevertheless, the fragments observed are also consistent with the major fragments in the CID of radical species (see above and SI). For OTSS, the three radical-induced fragments at *m/z* 898, 886, and 853 are still present and the relative intensity of tyrosine's sidechain loss is weak and similar to the one obtained by CID. Comparably, the

neutral losses S₂H[•] at *m/z* 939 are dominant as in the CID spectrum (Figure S3), which we hypothesize involves the shift of the radical from tyrosine to Cys1 C_α (Scheme 3). The fragmentation ratio of OTSS radical anion is very weak, close to the spontaneous fragmentation level, and does not significantly increase with the photon energy (Figure 3 inset).

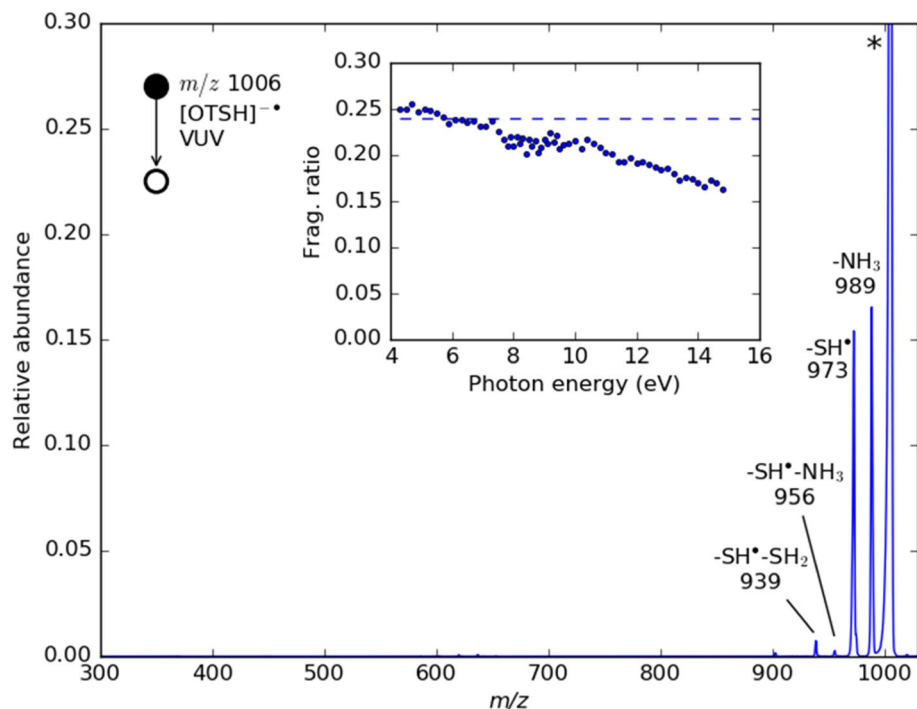
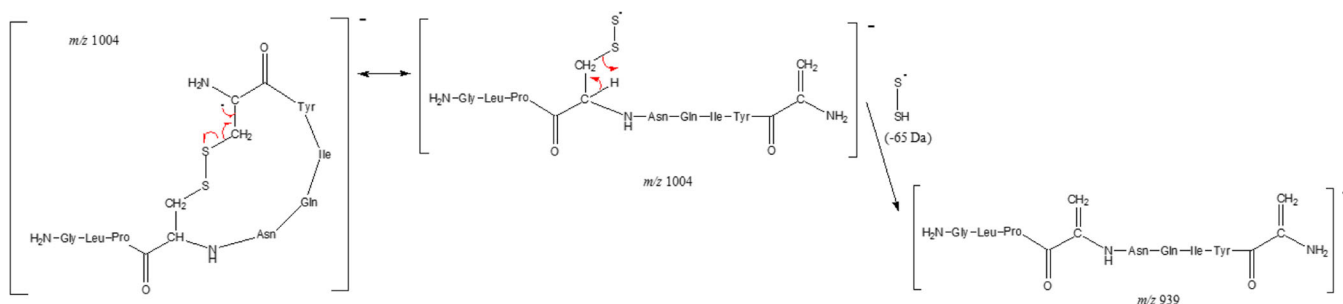


Figure 4. [OTSH]⁻ VUVPD mass spectrum averaged over the full 4.5 to 16 eV range. In inset, the evolution of the fragmentation ratio with the VUV photon energy (bullets), compared to the spontaneous fragmentation ratio (dashed line)



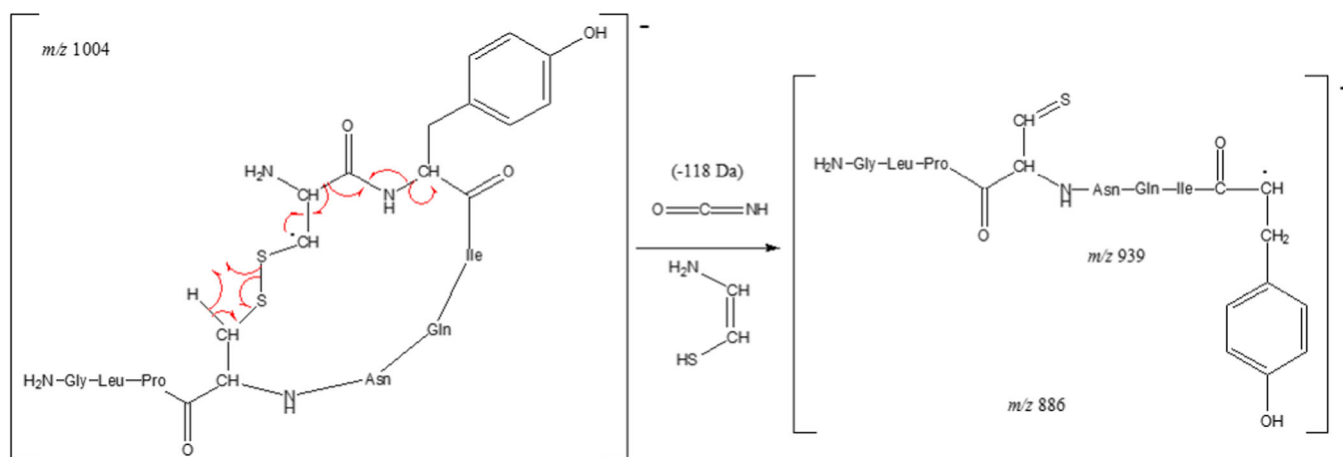
Scheme 3. Proposed mechanism for the loss of S_2H^\bullet from $[OTSS]^\bullet-$

For OTSH (Figure 4), the two radical-induced mechanisms leading to the loss of NH_3 and SH^\bullet are again predominant, supporting the presence and reactivity of thiyl radicals. No other fragment is significantly populated, so that all the fragmentation is generated around the radical centers on sulfur. The overall VUV fragmentation ratio is very high, around 25% (Figure 4 inset) and close to the spontaneous fragmentation level. It slightly decays with increasing photon energy.

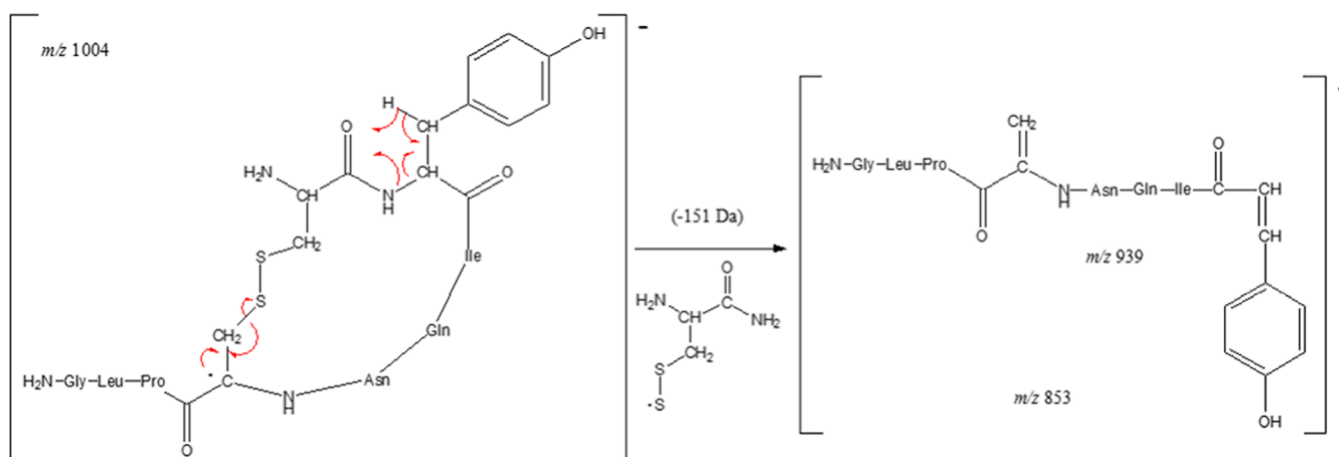
Discussion and Conclusions

In oxytocin, since the C-term is amidated, the most acidic sites are the free thiols (pKa 8.2–9.5) in OTSH and tyrosine (pKa 10.4) in OTSS. Thus, when the disulfide bridge is reduced, the free cysteines are the preferential sites for deprotonation. Given the low ionization energy of thiolates (~ 2 eV [32]), even a low-energy photon might form a radical by electron photodetachment from anionic cysteines. In the non-reduced oxytocin, the most probable site for deprotonation is tyrosine (a second deprotonation must occur on the backbone in the dianion). Here again, considering the low ionization energy of tyrosinate (~ 2.2 eV [32]), the radical will be formed on tyrosine. The fragmentation patterns observed are consistent with those localizations of the radicals, in particular the loss of the tyrosine sidechain in OTSS. However, the nature of fragments also indicates that the radical on tyrosine seems to be mobile and prone to move to the backbone via H abstraction,

e.g., from Cys1/Cys6 C_α or C_β , leading to the appearance of intense radical-induced fragments far from tyrosine, including SH^\bullet and S_2H^\bullet . Remarkably, the latter fragmentation is only observed from non-reduced OT and may reflect the presence of an intact disulfide bridge, consistent with the proposed formation mechanism. This indicates that the absorption of photons at 266 nm is not necessarily followed by the homolytic cleavage of existing disulfide bridges, in contrast to what was reported for positively charged ions [33]. In order to understand this difference, it is worth looking for comparison, at the mechanisms proposed to explain the S–S radical-induced bond cleavage by ECD/ETD in protonated peptides (see ref. 307–309 in [17]). All require proton-rich species: either neighboring positive charges induce the coulomb stabilization of the S–S σ^* orbital, which enables the direct capture of an electron by the disulfide bridge and its cleavage into thiyl and thiolate (the latter neutralized by an intramolecular proton transfer); or the electron attachment to a neighboring protonated site is followed by a H-atom transfer from the radical site to the disulfide bridge, inducing its barrierless cleavage into thiol and thiyl. In contrast, however, oxytocin anions are depleted in protons. The electron detachment occurs preferentially from the deprotonated tyrosine, thus there is no H available to transfer the radical away. As shown above, direct tyrosine radical fragmentation is observed. However, there is more than this fragmentation path, and the other fragments require different positions of the radical. The only possibility to shift the radical position away from tyrosine is a H-atom “back transfer” to the



Scheme 4. Proposed mechanism for the generation of ion at m/z 886 from $[OTSS]^\bullet-$



Scheme 5. Proposed mechanism for the generation of ion at m/z 853 from $[\text{OTSS}]^{-}$

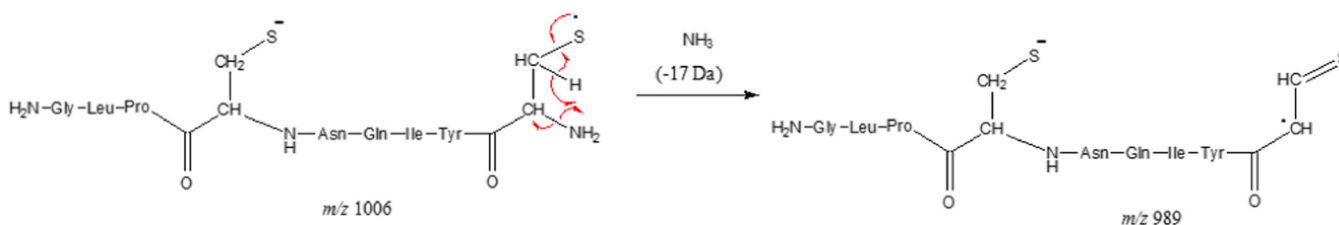
radical, which can only take place from H-containing sites, in particular the backbone. The OTSS radical fragmentation schemes proposed (Schemes 3, 4, and 5) start from radical positions on the backbone that implicitly incorporate an initial H-atom transfer to tyrosine. It is worth noting that the long VUV irradiation time opens the possibility for many rearrangements and possibly other radical re-localization on the backbone. Thus, the proposed fragmentation mechanisms represent one possibility to reach the observed fragments. In the case of OTSH and thiyl radicals, on the contrary, the reactivity leading to local fragmentation seems to exceed possible intramolecular H transfer such that no other radical-induced fragments are observed.

From CID analysis in the negative mode (see SI), the presence of the disulfide bridge of OTSS is supported by series of specific fragments [34, 35], in particular the S_2H^+ loss on the parent peptide (S_2H^+ loss for the radical) and the -2.016 Da shift on usual b/c/y-type fragments. Remarkably, the -2.016 Da shift does not appear in the OTSS radical. This can be explained by the more reactive radical-induced fragmentation mechanisms that decrease the proportion of classical backbone fragments. From the presence of those specific fragments, it can be reasonably inferred that the disulfide bridge is conserved in OTSS radical anion.

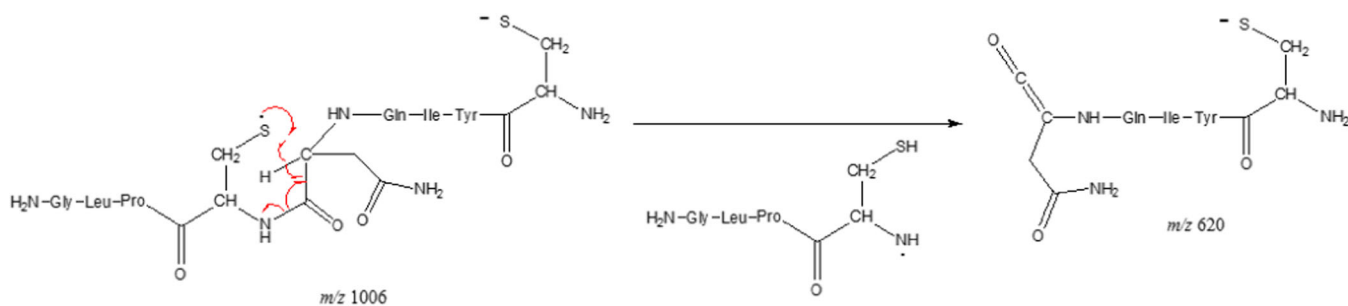
The analysis of the VUV photo-dissociation of oxytocin dianions indicates that their fragmentation is predominantly driven by the radical, as understood from fragmentation patterns similar to the CID of radical anions i.e. significantly different from non-radical anions. From this, it can be deduced that the absorption of VUV photons first induces electron detachment, and then the remaining internal energy may lead to the

fragmentation of the radical. All the fragmentation mechanisms proposed (Schemes 3, 4, 5, 6, and 7 and Scheme S1 to Scheme S5) start from the radical species. However, in terms of total fragmentation yield (including electron detachment), both OTSS and OTSH dianions are comparable, indicating that the presence of the disulfide bridge has surprisingly no major effect on the disappearance of dianions. Since the ionization energy of thiolate and tyrosinate is very close, no major difference was expected in terms of electron detachment. However, it can be noted that the relative abundance of the radical OT anion vs. fragments is drastically different: high in the case of OTSS and low for OTSH. This suggests that the radical anion of oxytocin is more prone to fragment when the disulfide bridge is open. This is consistent with the spontaneous fragmentation levels or radical anions measured without VUV. Eventually, in both cases, the increase of photon energy opens new ionization routes, reflecting in increased VUV photo-detachment cross section and as a result, increased secondary fragmentation.

Turning to the VUV fragmentation of radicals, one might observe that $[\text{OTSH}]^{-}$ presents a considerably higher fragmentation ratio than $[\text{OTSS}]^{-}$ and the dianions. As mentioned above, this is consistent with the very high spontaneous fragmentation ratio observed for OTSH radical (respectively low for OTSS radical). This represents the most striking difference between OTSS and OTSH radicals. One might argue that the low apparent fragmentation of $[\text{OTSS}]^{-}$ is due to invisible backbone fragmentations because of the presence of the disulfide bridge keeping fragments together. However, there is neither backbone fragmentation in the VUPD spectrum of $[\text{OTSH}]^{-}$ nor in the CID spectrum of $[\text{OTSS}]^{-}$. Thus, the hypothesized presence of a disulfide bridge is not likely to



Scheme 6. Proposed mechanism for the loss of NH_3 from $[\text{OTSH}]^{-}$



Scheme 7. Proposed mechanism for the formation of b_5 fragment ion from $[\text{OTSH}]^{\cdot-}$

artificially lower the apparent fragmentation ratio of $[\text{OTSS}]^{\cdot-}$. On the contrary, two other observations can be made: on the one hand, the comparison with CID spectra of non-radical anions suggests that the fragmentation of both OT radicals is essentially radical driven. On the other hand, fragmentation patterns are very different for $[\text{OTSS}]^{\cdot-}$ vs. $[\text{OTSH}]^{\cdot-}$, which suggests that the initial position of the radical in the anions, hypothesized on cysteine for OTSH but on tyrosine or the backbone in OTSS, is responsible for the nature of the fragments. Thus, the difference in fragmentation level between $[\text{OTSS}]^{\cdot-}$ and $[\text{OTSH}]^{\cdot-}$ most likely reflects the different intrinsic reactivity associated with the actual radical position in OT.

In terms of particular effects of VUV radiations on the radicals, it is worth reminding that the major effect of VUV is to ionize, as illustrated by the VUVPD mass spectrum of dianions. However, the ionization of radical anions yields neutral products. Thus, what is observed for radical anions is how spontaneous fragmentation is affected by VUV radiations. For OTSS radical, no particular effect is noticed: branching ratios remain constant and the overall fragmentation level remains very close to its spontaneous level. In the case of OTSH radical, however, the fragmentation level decreases with photon energy. The ionization cross section increases with VUV photon energy, as illustrated by the evolution of dianions VUV photo-detachment/photo-fragmentation yield. It seems that the ionization cross section of OTSH radical anion increases less rapidly than that of its fragments, resulting in the overall decrease of the apparent fragmentation ratio as a function of photon energy.

In conclusion, the analysis of the fragmentation patterns of oxytocin in both its reduced and non-reduced forms, for the anionic and radical anionic species, enabled the interpretation of the VUV photo-fragmentation spectra. Analyzing the nature of VUVPD fragments, it is significant that VUV fragments are identical to the major radical-induced fragments observed by CID: this suggests that the fragmentation does not occur in the excited state, but rather after redistribution of the energy deposited by either electron photon-detachment or collisions. The effect of VUV is, as expected, principally to ionize. Then, consecutive (secondary) fragmentation can be observed, as proven by the exclusive observation of radical-directed fragments. This secondary fragmentation is considerably enabled by the initial position of the radical, and the nature of the

fragments reflects the intrinsic fragmentation reactivity associated to the position of this radical. In particular, thiyl radicals seem to very efficiently lead to NH_3 and SH^\cdot loss in oxytocin, whereas the tyroxy radical is prone to induce an intramolecular H transfer and seems to be less efficiently coupled to a specific fragmentation path. Thus, the presence of the disulfide bridge does not seem so much to influence per se oxytocin's susceptibility to photo-fragment. However, the possibility to form a radical on free cysteines seems to increase the susceptibility of reduced oxytocin to photo-fragment after photo-ionization in the VUV. Interestingly, disulfide bridges, which are fundamental for protein structuration, could also be responsible for an increased resistance to ionizing radiations. Or, more precisely, denatured proteins with reduced disulfide bridges and free cysteines could be more sensitive to radiation damages via the photo-generation of reactive cysteine radicals.

Acknowledgments

We thank the general technical staff of SOLEIL for running the facility.

Funding Information

Research leading to these results received funding from the European Research Council under the European Union's Seventh Framework Programme (FP7/2007–2013 Grant Agreement No. 320659). SOLEIL support is acknowledged under project no. 20120093. This research was supported by the Agence Nationale de la Recherche Scientifique, France, under the project no. BLAN08-1_348053.

References

- O'Neill, P., Wardman, P.: Radiation chemistry comes before radiation biology. *Int. J. Radiat. Biol.* **85**, 9–25 (2009)
- Görner, H.: Photochemistry of DNA and related biomolecules: yields and consequences of photoionization. *J. Photochem. Photobiol. B.* **26**, 117–139 (1994)
- Wien, F., Miles, A.J., Lees, J.G., Vronning Hoffmann, S., Wallace, B.A.: VUV irradiation effects on proteins in high-flux synchrotron radiation circular dichroism spectroscopy. *J. Synchrotron Radiat.* **12**, 517–523 (2005)
- Giese, B.: Electron transfer in DNA. *Curr. Opin. Chem. Biol.* **6**, 612–618 (2002)
- Davies, M.J., Truscott, R.J.W.: Photo-oxidation of proteins and its role in cataractogenesis. *J. Photochem. Photobiol. B.* **63**, 114–125 (2001)

6. Giese, B., Napp, M., Jacques, O., Boudebous, H., Taylor, A.M., Wirz, J.: Multistep electron transfer in oligopeptides: direct observation of radical cation intermediates. *Angew. Chemie - Int. Ed.* **44**, 4073–4075 (2005)
7. Aubert, C., Vos, M.H., Mathis, P., Eker, A.P.M., Brettel, K.: Mechanism of radical transfer during photoactivation of the flavoprotein DNA photolyase. *Nature*. **405**, 586–590 (2000)
8. Stubbe, J.A., Nocera, D.G., Yee, C.S., Chang, M.C.Y.: Radical initiation in the class I ribonucleotide reductase: long-range proton-coupled electron transfer? *Chem. Rev.* **103**, 2167–2201 (2003)
9. Mishra, A.K., Chandrasekar, R., Klapper, M.H., Faraggi, M.: Long-range electron transfer in peptides. Tyrosine reduction of the indolyl radical: reaction mechanism, modulation of reaction rate, and physiological considerations. *J. Am. Chem. Soc.* **116**, 1414–1422 (1994)
10. Dean, R.T., Hunt, J.V., Grant, A.J., Yamamoto, Y., Niki, E.: Free radical damage to proteins: the influence of the relative localization of radical generation, antioxidants, and target proteins. *Free Radic. Biol. Med.* **11**, 161–168 (1991)
11. Hawkins, C.L., Davies, M.J.: Generation and propagation of radical reactions on proteins. *Biochim. Biophys. Acta Bioenerg.* **1504**, 196–219 (2001)
12. Haywood, J., Mozziconacci, O., Allegra, K.M., Kerwin, B.A., Schöneich, C.: Light-induced conversion of trp to gly and gly hydroperoxide in IgG1. *Mol. Pharm.* **10**, 1146–1150 (2013)
13. Creed, D.: The photophysics and photochemistry of the near-UV absorbing amino-acids - III. Cystine and its simple derivatives. *Photochem. Photobiol.* **39**, 577–583 (1984)
14. Everett, S.A., Schöneich, C., Stewart, J.H., Asmus, K.D.: Perthiyl radicals, trisulfide radical ions, and sulfate formation. A combined photolysis and radiolysis study on redox processes with organic di- and trisulfides. *J. Phys. Chem.* **96**, 306–314 (1992)
15. Mason, B.D., Schöneich, C., Kerwin, B.A.: Effect of pH and light on aggregation and conformation of an IgG1 mAb. *Mol. Pharm.* **9**, 774–790 (2012)
16. Wang, W., Singh, S., Zeng, D.L., King, K., Nema, S.: Antibody structure, instability, and formulation. *J. Pharm. Sci.* **96**, 1–26 (2007)
17. Simons, J.: Molecular anions. *J. Phys. Chem. A.* **112**, 6401–6511 (2008)
18. Osburn, S., Burgie, T., Berden, G., Oomens, J., O'Hair, R.A.J., Ryzhov, V.: Structure and reactivity of homocysteine radical cation in the gas phase studied by ion-molecule reactions and infrared multiple photon dissociation. *J. Phys. Chem. A.* **117**, 1144–1150 (2013)
19. Leslie, M., Lau, J.K.C., Lawler, J.T., Siu, K.W.M., Steinmetz, V., Maître, P., Hopkinson, A.C., Ryzhov, V.: Cysteine radical/metal ion adducts: a gas-phase structural elucidation and reactivity study. *Chem. Aust.* **81**, 444–452 (2016)
20. Parker, W.R., Holden, D.D., Cotham, V.C., Xu, H., Brodbelt, J.S.: Cysteine-selective peptide identification: selenium-based chromophore for selective S–Se bond cleavage with 266 nm ultraviolet photodissociation. *Anal. Chem.* **88**, 7222–7229 (2016)
21. Diedrich, J.K., Julian, R.R.: Site selective fragmentation of peptides and proteins at quinone modified cysteine residues investigated by ESI-MS. *Anal. Chem.* **82**, 4006–4014 (2010)
22. Brunet, C., Antoine, R., Allouche, A.-R., Dugourd, P., Canon, F., Giuliani, A., Nahon, L.: Gas phase photo-formation and vacuum UV photofragmentation spectroscopy of tryptophan and tyrosine radical-containing peptides. *J. Phys. Chem. A.* **115**, 8933–8939 (2011)
23. Meyer-Lindenberg, A., Domes, G., Kirsch, P., Heinrichs, M.: Oxytocin and vasopressin in the human brain: social neuropeptides for translational medicine. *Nat. Rev. Neurosci.* **12**, 524–538 (2011)
24. Mozziconacci, O., Schöneich, C.: Photodegradation of oxytocin and thermal stability of photoproducts. *J. Pharm. Sci.* **101**, 3331–3346 (2012)
25. Hoffman, M.Z., Hayon, E.: One-electron reduction of the disulfide linkage in aqueous solution. Formation, protonation, and decay kinetics of the RSSR– radical. *J. Am. Chem. Soc.* **94**, 7950–7957 (1972)
26. Tung, T.-L., Stone, J.A.: The formation and reactions of disulfide radical anions in aqueous solution. *Can. J. Chem.* **53**, 3153–3157 (1975)
27. Milosavljević, A.R., Nicolas, C., Gil, J.-F., Canon, F., Réfrégiers, M., Nahon, L., Giuliani, A.: VUV synchrotron radiation: a new activation technique for tandem mass spectrometry. *J. Synchrotron Radiat.* **19**, 174–178 (2012)
28. Nahon, L., de Oliveira, N., Garcia, G.A., Gil, J.-F., Pilette, B., Marcouillé, O., Lagarde, B., Polack, F.: DESIRS: a state-of-the-art VUV beamline featuring high resolution and variable polarization for spectroscopy and dichroism at SOLEIL. *J. Synchrotron Radiat.* **19**, 508–520 (2012)
29. Brunet, C., Antoine, R., Dugourd, P., Canon, F., Giuliani, A., Nahon, L.: Formation and fragmentation of radical peptide anions: insights from vacuum ultra violet spectroscopy. *J. Am. Soc. Mass Spectrom.* **23**, 274–281 (2012)
30. Milosavljević, A.R., Nicolas, C., Lemaire, J., Dehon, C., Thissen, R., Bizau, J.-M., Réfrégiers, M., Nahon, L., Giuliani, A.: Photoionization of a protein isolated in vacuo. *Phys. Chem. Chem. Phys.* **13**, 15432–15436 (2011)
31. Sohn, C.H., Gao, J., Thomas, D.A., Kim, T.-Y., Goddard III, W.A., Beauchamp, J.L.: Mechanisms and energetics of free radical initiated disulfide bond cleavage in model peptides and insulin by mass spectrometry. *Chem. Sci.* **6**, 4550–4560 (2015)
32. Ganisl, B., Valovka, T., Hartl, M., Taucher, M., Bister, K., Breuker, K.: Electron detachment dissociation for top-down mass spectrometry of acidic proteins. *Chem. - A Eur. J.* **17**, 4460–4469 (2011)
33. Agarwal, A., Diedrich, J.K., Julian, R.R.: Direct elucidation of disulfide bond partners using ultraviolet photodissociation mass spectrometry. *Anal. Chem.* **83**, 6455–6458 (2011)
34. Bilusich, D., Bowie, J.H.: Fragmentation of (M-H)⁻ anions of underivatized peptides. Part 2: characteristic cleavages of Ser and Cys and of disulfides and other post-translational modifications, together with some unusual internal processes. *Mass Spectrom. Rev.* **28**, 20–34 (2009)
35. Thakur, S.S., Balaram, P.: Fragmentation of peptide disulfides under conditions of negative ion mass spectrometry: studies of oxidized glutathione and contryphan. *J. Am. Soc. Mass Spectrom.* **19**, 358–366 (2008)